Use of a Lowest Intensity [241]Am Compton Spectrometer for the Measurement of Directional Compton Profiles of ZnSe

Babu Lal Ahuja and Narayan Lal Heda

Department of Physics, University College of Science, M. L. Sukhadia University, Udaipur 313001, Rajasthan, India

Reprint requests to Dr. B. L. A.; E-mail: blahuja@yahoo.com

In this paper we report on electron momentum densities in ZnSe using Compton scattering technique. For the directional measurements we have employed a newly developed 100 mCi [241]Am Compton spectrometer which is based on a small disc source with shortest geometry. For the theoretical calculations we have employed a self-consistent Hartree-Fock linear combination of atomic orbitals (HF-LCAO) approach. It is seen that the anisotropy in the measured Compton profiles is well reproduced by our HF-LCAO calculation and the other available pseudopotential data. The anisotropy in the Compton profiles is explained in terms of energy bands and bond length. – PACS numbers: 13.60.Fz, 78.70. Ck, 78.70.-g

Key words: Compton Scattering; Electron Momentum Density; Band Structure Calculation; II-VI Semiconductor.

1. Introduction

ZnSe is a II-VI semiconductor with a band gap of 2.7 eV. Such a large direct band gap semiconductor is a prime candidate for blue and ultraviolet light-emitting diodes, ultraviolet photodetectors, lasers etc. [1, 2]. Due to the wide applications of ZnSe, many workers have reported theoretical and experimental work on it that mainly includes optical properties, band structure calculations, neutron powder diffraction, electron mobility, photoluminescence, isotropic Compton profiles etc., see for example [3 – 8].

It is well established that Compton scattering studies of compounds can reveal valuable information about the conduction electrons through an analysis of the Compton line shape, see [9] for a comprehensive review of the subject. The Compton profile $J(p_z)$ derived from the measured differential scattering cross-section is simply a projection of the electron momentum density $n(\vec{p})$ along the scattering vector (assigned as the z-axis). It is defined as

$$J(p_z) = \int \int n(\vec{p}) \mathrm{d}p_x \mathrm{d}p_y. \qquad (1)$$

The extraction of the profile from the observed spectrum involves several corrections, the most problematical being that for multiple scattering, bremsstrahlung contribution and failure of impulse approximation. In order to circumvent these difficulties, the Compton profiles are mainly interpreted in terms of the difference between pairs of directional profiles, i. e.

$$\Delta J(p_z) = J_{hkl}(p_z) - J_{h'k'l'}(p_z), \qquad (2)$$

where hkl and $h'k'l'$ denote planes perpendicular to the scattering vector. Since $\Delta J(p_z)$ is relatively immune to systematic errors, the anisotropy in the momentum densities provides a very useful test of the electronic structure theories.

In spite of the use of synchrotron radiations (which is very expensive and limited) in Compton spectroscopy, there is still a need for laboratory sources like [241]Am (half life 432.2 years). Probably due to the problems of radiation shielding and lower efficiency of the solid state detectors at high energies like that from [198]Au, ^{137}Cs, only a limited number of high energy Compton spectrometers have been fabricated so far, see for example [10, 11]. During the last two decades, most of the γ-ray Compton scattering studies were based on annular [241]Am sources, see for example [9] and [12]. Unfortunately, the use of annular γ-emitting sources in the measurement of directional Compton profiles is complicated because in such arrangements the scattering vector $(\vec{k})$ lies anywhere on the surface of a cone of semi-angle of the

order $1/2(180° - θ)$, where $θ$ is the scattering angle. In addition, the beam divergencies cause $θ$ to be distributed on a family of cones with varying conic angles. This high degree of imprecision in $\vec{k}$ may be irrelevant in the study of Compton profiles of polycrystalline samples, but it presents a serious problem in the directional momentum densities. Therefore, a collimated planar geometry with a small disc type source is very helpful in the measurement of directional Compton profiles. In this paper we present the first ever directional Compton profiles of ZnSe, measured along the [100] and [110] directions, using the lowest intensity ^{241}Am Compton spectrometer. To compare our experimental data we have also computed the directional Compton profiles by the linear combination of atomic orbitals (LCAO), using the Hartree-Fock (HF) scheme of the CRYSTAL03 code [13]. In this paper, we have used atomic units (a.u.) where $e = m = \hbar = 1$, $c = 137.036$ and the SI equivalent of 1 a.u. of momentum is $1.99289 \cdot 10^{-24}$ kg m s^{-1}.

2. HF-LCAO Calculation

We have carried out band structure calculations for the computation of directional Compton profiles, energy bands and the density of states of ZnSe by the HF-LCAO scheme of CRYSTAL03 [13]. In the LCAO technique, the Bloch functions of the crystalline orbitals (CO's), built from the local atom centred Gaussian functions, are the solutions of one-electron equations. HF is a ground state formulation for the treatment of an inhomogeneous, interacting electronic distribution and is therefore applicable to the Compton scattering studies of the ground state momentum densities. The HF operator is defined as

$$\hat{H}_{HF} = \hat{T} + \hat{V} + \hat{C} + \hat{X}_{HF}. \tag{3}$$

$\hat{T}$, $\hat{V}$, $\hat{C}$, and $\hat{X}_{HF}$ are the kinetic, external potential, Coulomb and exchange operators, respectively. In the HF approach there is an exact exchange interaction between the electrons, while the electron correlation effects are not considered. Therefore, to incorporate the electron correlation effects in our calculation, we have incorporated the Von Berth-Hedin (VBH) form of the density functional [13]. The all-electron basis sets for Zn^{2+} and Se^{2-}, taken from [14, 15], were re-optimized for the present zincblende structure of ZnSe. Following the standard truncation criteria of the code, the calculations were carried out to self-consistence using

120 points in the irreducible wedge of the first Brillouin zone, taking advantage of the symmetry.

Since the binding energies of the K shell in Zn and Se are 9.658 and 12.657 keV, in the present set-up these electrons do not contribute to the Compton phenomena beyond $+2.24$ and -2.49 a.u., respectively. While calculating the total theoretical profiles, the contribution of 1s^2 electrons of Zn was taken up to 2.24 a.u. only. On the other hand, 1s^2 electrons of Se do not contribute to the Compton profile range (0 – 7 a.u.) considered here. Therefore, after taking care of the K shell contributions, the total theoretical profiles of ZnSe were normalized to 26.97 electrons in the momentum range 0 – 7 a.u.

3. Experiment

3.1. ^{241}Am Compton Spectrometer and Test Data

The layout of our newly designed, fabricated and commissioned planar ^{241}Am Compton spectrometer which employs a disc source is shown in Figure 1a. The 100 mCi γ-emitting point source was procured from M/s Chemotrade, Germany. The distances between the source to the sample (s-s) and the sample to the detector (s-d) were 5.7 and 8.8 cm, respectively. In earlier conventional 200 – 300 mCi planar Compton spectrometers the s-s and s-d distances were almost double of our distances [9]. Considering various aspects, like requirement of a better resolution, higher Compton count rate, tolerance of larger divergence at the higher angles, fulfillment of impulse approximation criteria, a scattering angle of 165° was chosen. The total experimental momentum resolution ($Δp_z$) consists of two main parts related to energy broadening of the detector and geometrical broadening of the spectrometer:

$$Δp_z = \sqrt{\underbrace{\left(\left(\frac{∂p_z}{∂ω_2}\right)Δω_2\right)^2}_{\text{detector}} + \underbrace{\left(\left(\frac{∂p_z}{∂θ}\right)Δθ\right)^2}_{\text{geometry}}}. \tag{4}$$

In our set-up, the resolution of the detector [first part of the right hand side of (4)] corresponds to a momentum resolution of 0.545 a.u. [Gaussian full width at half maximum (fwhm)] while the resolution arising from the angular divergence [second part of (4)] comes to about 0.079 a.u. The angular divergence [$Δθ$ in (4)] was determined by simulating the path of the incident and the scattered photons using Monte Carlo routine.
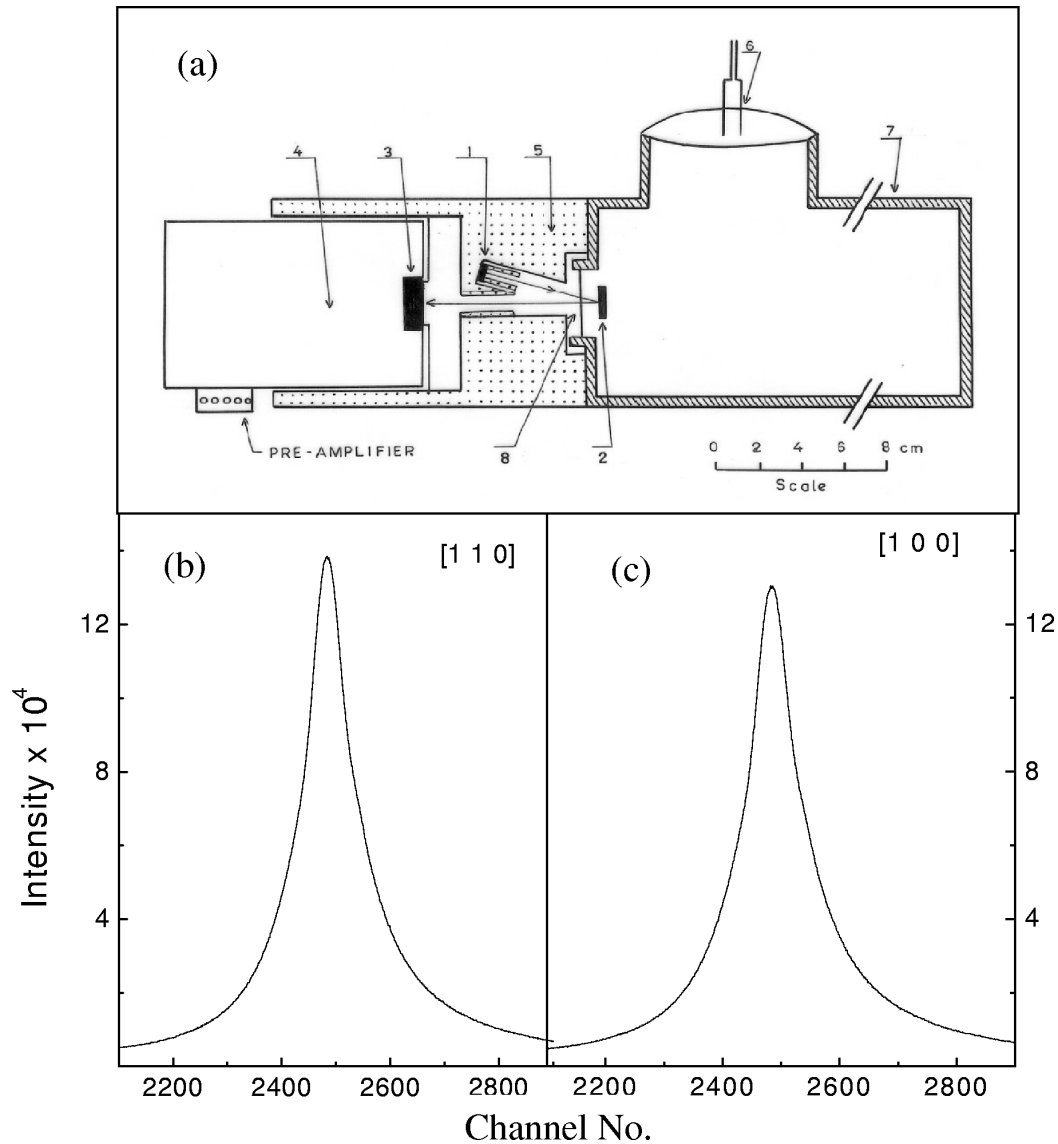
Fig. 1. (a) Layout of the 100 mCi ^{241}Am Compton spectrometer. The dotted region shows the lead shielding. Shown are: 100 mCi ^{241}Am disc source with active dimension 0.4 cm diameter and 0.12 cm length (1), sample position (2), Ge detector crystal (3), HPGe detector capsule (4), lead shielding around the source and the detector (5), port for evacuation (6), scattering chamber (diameter 10 cm, length 30 cm and wall thickness 0.5 cm) made of brass (7) and Mylar foil (25 μm) to evacuate the scattering chamber (8). The associated electronics like high voltage power supply, spectroscopy amplifier, analog-to-digital converter, multichannel analyzer are not shown. (b) Energy spectrum of Compton scattering from a ZnSe single crystal grown along the [110] direction. (c) Same as (b) except the crystalline direction which is now [100].

Therefore the overall momentum resolution (Δp_z) of the present spectrometer comes out to be 0.55 a.u.

To test the applicability of the spectrometer, a test run on sample Al was made for a period of 21.22 h. The raw data from the measurement on Al were processed to remove the background and to correct for the energy dependence of the scattering cross-section and absorption in the sample. The spectrum was also partially deconvoluted to remove the asymmetric low energy tail of the detector response function following the approach of the Warwick group [9, 16]. The data were than converted into the momentum scale

and normalized to the free atom profile area. To remove the effect of multiple scattering events, up to the triple scattering contribution the profile was calculated by the Monte Carlo program of Felsteiner et al. [17]. The duly corrected data on Al were compared with the APW (augmented plane wave) theoretical profile [18] after convoluting it with a Gaussian fwhm of 0.55 a.u. An excellent agreement between the experimental values [(0.339 ± 0.002), (0.210 ± 0.001), (0.142 ± 0.001) and (0.100 ± 0.001) e/a.u. at $p_z = 4.0$, 5.0, 6.0 and 7.0, respectively] with the corresponding APW theoretical values (0.324, 0.200, 0.133 and 0.097 e/a.u.) shows the correctness of the design of our Compton spectrometer, the data reduction and its applications in the measurement of Compton profiles for a variety of materials.

3.2. Directional Profiles of ZnSe

Two identical samples (thickness 2 mm and diameter 15 mm) of ZnSe, grown along the [100] and [110] directions, were procured from M/s Cradley Crystals, Russia. The orientations of the samples were checked by Laue photographs and were found to be aligned to within $\pm 1°$. During separate measurements, the samples were mounted in a scattering chamber in such a way that $\vec{k}$ was exactly along the direction of the crystals. During the exposure of about 185 and 196 h, about 25.2 and 26.6 million counts were accumulated in the Compton profile region (-10 to $+10$ a.u.) for the directions [100] and [110], respectively. The raw Compton data, which look similar for both orientations, are shown in Figs. 1b and 1c. Both experimental data were improved by various corrections, as mentioned earlier. The experimental profiles were normalized to 26.97 electrons as mentioned in Section 2.

4. Results and Discussion

In Fig. 2, the unconvoluted HF-LCAO and our experimental Compton profiles for the [100] and [110] directions are plotted. In the vicinity of $J(0)$ our experimental profiles are slightly lower than the theoretical profiles. Instead of comparing the total profiles, we compared the anisotropic profiles, where some systematic deviations, as discussed earlier, are minimized both in the experiment and the theory. In order to account for the experimental resolution, the theoretical profiles were convoluted with a Gaussian fwhm of 0.55 a.u. In Fig. 3, the anisotropies between the above two directions from our theoretical HF pro-
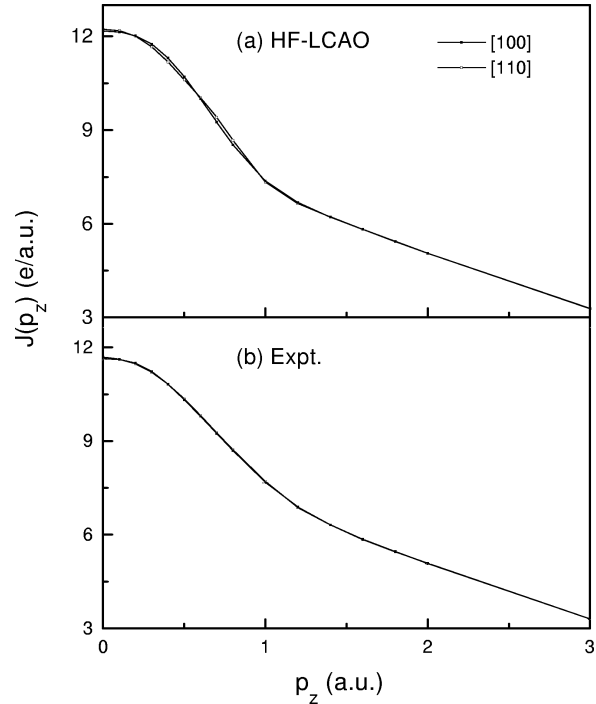

Fig. 2. Absolute Compton profiles for ZnSe along [100] and [110] directions from (a) unconvoluted HF-LCAO calculation and (b) present experiment. In the experiment, the errors ($\pm \sigma$) are within the size of the symbols used.

files (convoluted) as well as these of our experimental profiles are plotted. Also incorporated here is the anisotropy derived from the pseudopotential calculations of Nara et al. [19]. It is seen that the oscillations in the directional differences (ΔJ) from the experimental and both the theoretical calculations are quite similar; although near $J(0)$ the pseudopotential calculations [19] underestimate the anisotropy in the momentum density. It is evident from this comparison that the anisotropy, measured using the present spectrometer, provides a good testing ground for the band structure calculations. The energy bands and density of states (DOS), as calculated from the present scheme, are plotted in Figure 4. There is a fairly good agreement between the topology of our calculated energy bands and that due to the GW (where G is the Green function and W the screened Coulomb interaction) approximation reported by Luo et al. [5] and the linearized APW calculation of Persson and Zunger [20]. Here the low lying bands (near -1.0 Hartree) come mainly from Zn 3d, Se 4sp and their polarized states. Separately, we have seen that these states also show their contribution in the formation of bands on the high energy side
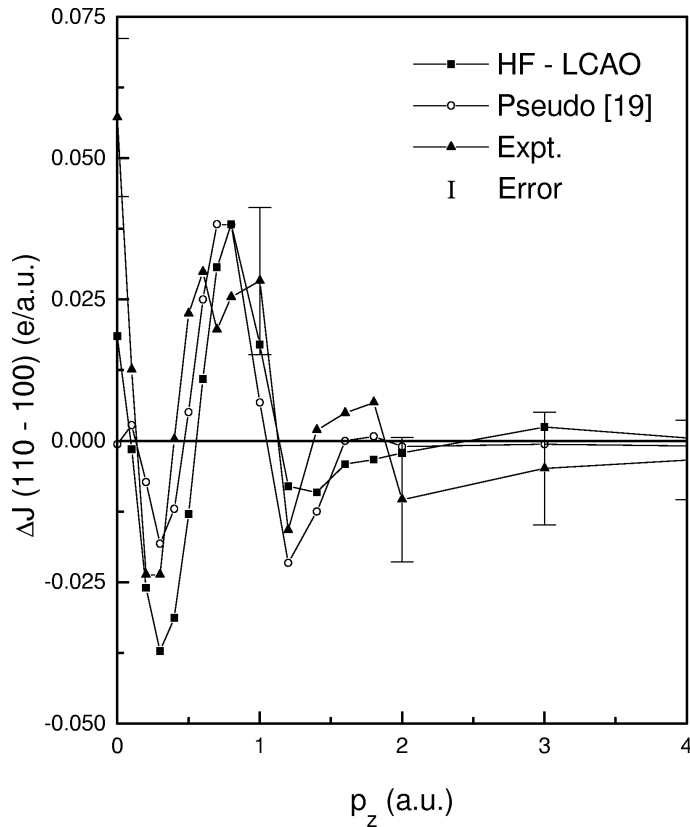
Fig. 3. Experimental and HF theoretical difference Compton profiles $J_{110}-J_{100}$ of ZnSe. Also included is the anisotropy derived from the pseudopotential calculation of Nara et al. [19]. Before computing the anisotropies, all the theoretical profiles were convoluted with a Gaussian fwhm of 0.55 a.u.

(near $+1.5$ Hartree). The periodicity in anisotropies (Fig. 3) can be partly explained on the basis of energy bands and DOS, as shown in Figure 4. The contribution of the momentum densities in the J_{100} can be depicted mainly by the energy bands and the degenerate states of the Δ branch. As can be seen from the DOS also, in this branch, the core and 3d electrons are on the lower energy side (< -0.80 Hartree), so their contribution to the total $n(\vec{p})$ is smooth. In the Δ branch there are several degenerate states at the X point which enhance the momentum density at the X point (ΓX $= 0.293$ a.u.). On the other hand, the major contribution in J_{110} arises from the energy bands and the degenerate states of the Σ branch. At the point Γ of this branch, there are also several degenerate states which give a higher momentum density in the vicinity of $p_z = 0$. Further, due to a large number of allowed states at the point U/K of this branch, there will be more momentum density at ΓK distances ($n \cdot 0.311$ a.u., where $n = 1, 2, 3...$). The oscillations in the anisotropy, as found in Fig. 3, are also consistent with the energy bands. The positive values of $J_{110} -$

J_{100} near $p_z = 0$ a.u. are due to the higher momentum density at the Γ point of the Σ branch, while the negative oscillation at about 0.3 a.u. is due to the degenerate states in the Δ branch. Further, the positive oscillation at about $p_z = 0.7$ a.u. is due to the higher momentum density at ΓK distance ($n \cdot 0.311$ a.u., where $n = 2$). Due to cancellation effects in $J_{110}-J_{100}$ and limitation of experimental resolution, few structures may not be visible in the anisotropy. Further, a complete cycle in the experimental anisotropy near $p_z = 1.2$ a.u. can be explained by the bond oscillation principle [21], which mentions that the Compton profiles and the momentum densities associated with the chemical bonds will exhibit oscillations along the bonding direction with a period $2\pi/b$, where b is the bond length. From this cycle, taking a period of oscillation as 1.2 a.u., we get the bond length as (5.24 ± 0.18) a.u., which is close to the theoretical value of the Se-Zn bond length (4.64 a.u.). It is worth mentioning here that the measurement of such small anisotropies in the momentum densities of ZnSe using the present spectrometer was possible due to the well-defined direction of the scattering vector.
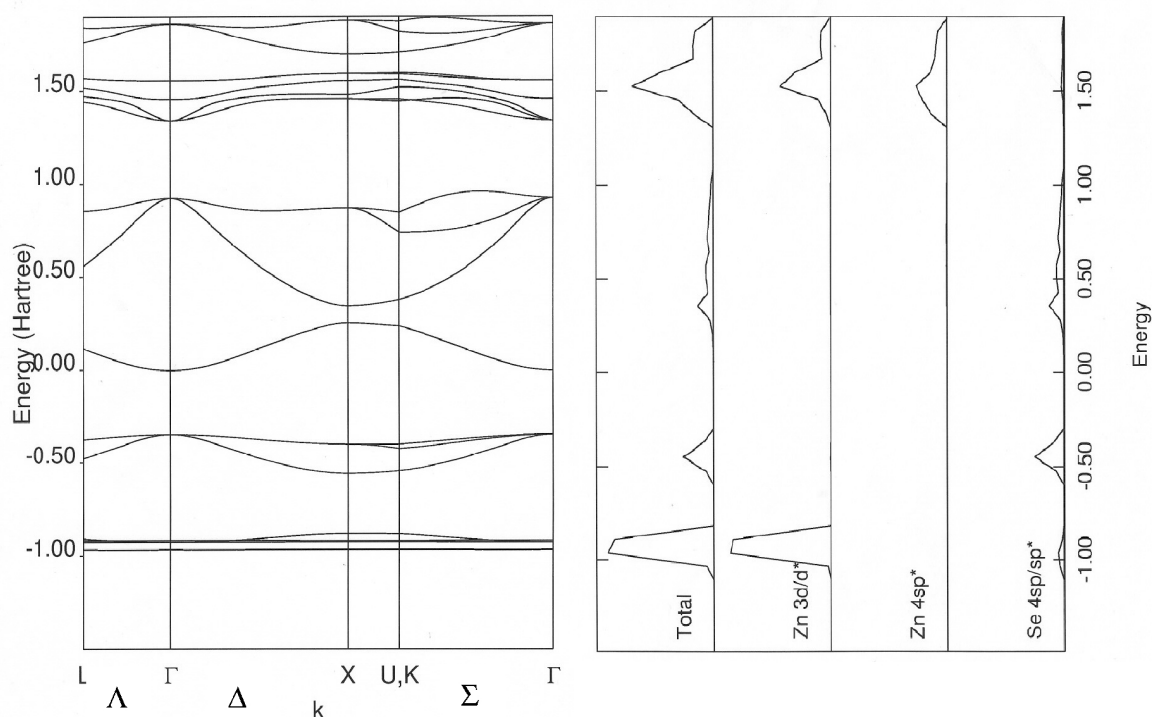
Fig. 4. Selected energy bands (E-k relation) of ZnSe along high symmetry directions of the first Brillouin zone. On the right hand side, the total and partial density of states (DOS) within the present HF-LCAO scheme are shown. The finite value of the density of states between few gaps in the E-k relation appears due to existence of energy bands in the other branches, which are not shown here. In atomic units, the unit of energy is Hartree. The positions of Γ, L, X and K/U vertices correspond to (0, 0, 0), (1/4, 1/4, 1/4), (0, 1/2, 0) and (3/8, 3/8, 0), respectively.

Using the present set-up, the measurements on relatively small single crystals (say, diameter about 5 mm) can also be made by collimating the incident and the scattered beams.

5. Conclusions

In conclusion it is evident that a careful design of a Compton spectrometer with a very weak source like 100 mCi is quite useful for the determination of anisotropies in the momentum densities. The first ever suggested design, which is based on drastically reduced source-sample and sample-detector distances, may be regarded as a guideline for such planar spectrometers. The resulting agreement between the HF-LCAO results and the directional Compton experiments for ZnSe is marginally better than that for the pseudopotential. The importance of this work lies in the fact that energy bands of semiconductors like the present one can be verified by directional Compton measurements. Moreover, the bond length can also be obtained from such measurements.

[1] D. B. Laks, C. G. Van de Walle, G. F. Neumark, and S. T. Pantelides, Phys. Rev. Lett. **66**, 648 (1991).

[2] G.-D. Lee, M. H. Lee, and J. Ihm, Phys. Rev. B **52**, 1459 (1995); E. Momroy, F. Omnes, and F. Calle, Semicond. Sci. Technol. **18**, R33 (2003).

[3] M. Oshikiri and F. Aryasetiawan, Phys. Rev. B **60**, 10754 (1999).

[4] U. Pietsch, J. Stahn, J. Davaasambuu, and A. Pucher, J. Phys. Chem. Solids **62**, 2129 (2001); J. Davaasambuu, A. Daniel, J. Stahn, and U. Pietsch, J. Phys. Chem. Solids **62**, 2147 (2001).

[5] W. Luo, S. I. Beigi, M. L. Cohen, and S. G. Louie, Phys. Rev. B **66**, 195215 (2002).

[6] A. Fleszar and W. Hanke, Phys. Rev. B **71**, 045207 (2005).

[7] P. F. Peterson, Th. Proffen, I.-K. Jeong, S. J. L. Billinge, K.-S. Choi, M. G. Kanatzidis, and P. G. Radaelli, Phys. Rev. B **63**, 165211 (2001); N. Avdonin, D. D. Nedeoglo, N. D. Nedeoglo, and V. P. Sirkeli, Phys. Status Solidi B **238**, 45 (2003); G. Neu, E. Tournie, C. Morhain, M. Teisseire, and J.-P. Faurie, Phys. Rev. B **61**, 15789 (2000).

[8] B. K. Panda and H. C. Padhi, Phys. Status Solidi B **166**, 519 (1991).

[9] M. J. Cooper, Rep. Prog. Phys. **48**, 415 (1985) and references therein; M. J. Cooper, P. E. Mijnarends, N. Shiotani, N. Sakai, and A. Bansil, X-Ray Compton Scattering, Oxford Science Publications, New York 2004.

[10] A. Andrejczuk, E. Zukowski, L. Dobrzynski, and M. J. Cooper, Nucl. Instrum. Methods A **337**, 133 (1993) and references therein.

[11] B. L. Ahuja, M. Sharma, and S. Mathur, Nucl. Instrum. Methods B **244**, 419 (2006) and references therein;

R. Vijayakumar, Shivaramu, L. Rajasekaran, N. Ramamurthy, and M. J. Ford, Nucl. Instrum. Methods B **234**, 185 (2005).

[12] B. K. Sharma and B. L. Ahuja, Phys. Rev. B **38**, 3148 (1988); S. Perkkio, S. Manninen, and T. Paakkari, Phys. Rev. B **40**, 8446 (1989); K. B. Joshi, R. Jain, R. K. Pandya, B. L. Ahuja, and B. K. Sharma, J. Chem. Phys. **111**, 163 (1999).

[13] V. R. Saunders, R. Dovesi, C. Roetti, R. Orlando, C. M. Zicovich-Wilson, N. M. Harrison, K. Doll, B. Civalleri, I. J. Bush, Ph. D'Arco, and M. Llunell, CRYSTAL2003 User's Manual, University of Torino, Torino 2003; M. D. Towler, A. Zupan, and M. Causa, Comp. Phys. Commun. **98**, 181 (1996).

[14] R. Franco, P. M. Sanchez, J. M. Recio, and R. Pandey, Phys. Rev. B. **68**, 195208 (2003).

[15] http://www.tcm.phy.cam.ac.uk/˜mdt26/crystal.html

[16] D. N. Timms, PhD Thesis, University of Warwick, England 1989.

[17] J. Felsteiner, P. Pattison, and M. J. Cooper, Phil. Mag. **30**, 537 (1974).

[18] N. I. Papanicolaou, N. C. Bacalis, and D. A. Papaconstantopoulos, Handbook of Calculated Electron Momentum Distributions, Compton Profiles and X-Ray Form Factors of Elemental Solids, CRC Press, London 1991.

[19] H. Nara, T. Kobayasi, and K. Shindo, J. Phys. C: Solid State Phys. **17**, 3967 (1984); T. Kobayasi, Private Communication (2004).

[20] C. Persson and A. Zunger, Phys. Rev. B **68**, 073205 (2003).

[21] B. Williams (Ed.), Compton Scattering, McGraw-Hill, London 1977.